



CHORUS

This is the accepted manuscript made available via CHORUS. The article has been published as:

Multiple-photon excitation of nitrogen vacancy centers in diamond

Peng Ji, R. Balili, J. Beaumariage, S. Mukherjee, D. Snoke, and M. V. Gurudev Dutt

Phys. Rev. B **97**, 134112 — Published 17 April 2018

DOI: [10.1103/PhysRevB.97.134112](https://doi.org/10.1103/PhysRevB.97.134112)

Multiple-photon excitation of nitrogen vacancy center in diamond

Peng Ji*

Department of Physics and Astronomy, University of Pittsburgh, Pittsburgh PA

R. Balili†

Department of Physics and Astronomy, Calvin College, Grand Rapids MI

J.Beaumariage, S.Mukherjee, D. Snoke, and M. V. Gurudev Dutt‡

Department of Physics and Astronomy, University of Pittsburgh, Pittsburgh PA, 15260

(Dated: April 5, 2018)

We report the observation of multi-photon photoluminescence excitation (PLE) below the resonant energies of nitrogen vacancy (NV) centers in diamond. The quadratic and cubic dependence of the integrated fluorescence intensity as a function of excitation power indicate a two-photon excitation pathway for the NV^- charge state and a three-photon process involved for the neutral NV^0 charge state respectively. Comparing the total multi-photon energy with its single-photon equivalent, the PLE spectra follows the absorption spectrum of single photon excitation. We also observed that the efficiency of photoluminescence for different charge states, as well as the decay time constant, was dependent on the excitation wavelength and power.

INTRODUCTION

The demonstration of single photon generation [1] and optical preparation and readout out of spin [2] in diamond nitrogen-vacancy centers (NV), coupled with its unique combination of features such as biocompatibility, stability, sensitivity to magneto-electric fields and long spin coherence, has launched diamond to prominence with regards to applications for nanoscale biological sensing and carbon-based quantum technology [3, 4]. Due to an efficient absorption in the visible region, around 450 nm to 575 nm for both the NV^0 and NV^- states [3], the electronic states of the electrons trapped in the NV defect centers are often prepared by non-resonantly exciting diamond with single photons using green light (520-540 nm). A resonant excitation of NV^- zero-phonon line (ZPL) at 638 nm (1.945 eV) to photo-ionize an electron and convert the NV to its neutral charge state via an absorption of two photons followed by an Auger process has also been reported [5]. Below resonance excitation at 1064 nm, half the energy of the usual green light excitation, has been used to study nonlinear photo-physical processes [6] and charge state dynamics [7, 8]. An interesting feature observed in these works was the spin-dependent signal that is emitted when simultaneously exciting with near infra-red and visible light, a phenomenon that is not well understood. Although the multi-photon photoluminescence excitation (PLE) experiment has been implemented in a wavelength range between 800 nm to 1040 nm [9], to the best of our knowledge, multi-photon PLE experiment has not been extended across the 2-photon (2P) resonance of NV^0 and NV^- . It is important to note that multiple-photon excitation is extremely advantageous for biological imaging and quantum information processing as it widely separates

the signal fluorescence from excitation.

In this work, we report our PLE measurement of NV photoluminescence using multi-photon excitation with pulsed light in the near-infrared range, 1050-1300 nm (0.95-1.18 eV). We discuss the different PL yields of NV at these excitation wavelengths. We also compare the time-resolved fluorescence decay of the NV excited states at various excitation energies and pump powers to shed light on the important features of the defect states.

EXPERIMENTAL SETUP

The sample in our experiments is micro-diamond crystals (High pressure high temperature synthesized 10-100 μm from Columbus Nanoworks. Nitrogen concentration: ~ 100 ppm). The NV ensembles investigated in these crystals are produced by electron irradiation and subsequent annealing. A laser pump, illuminating about 1 μm spot size on these crystals, yields sufficient fluorescence signal to noise ratio despite of an inherently low multi-photon excitation efficiency. An Optical Parametric Amplifier (Coherent OPA 9400) pumped by an amplified Ti:Sapphire laser system is used to provide 200 ps pulses, about 30 nm FWHM bandwidth at 250 kHz repetition rate, in the wavelength range used for the experiments. The “signal” output of the OPA can be tuned from 500 to 700 nm for non-resonant single-photon excitation while the “idler” covers the excitation wavelengths between 1000 to 2000 nm. A 0.8NA objective is used to both focus the pump beam onto the sample and collect the diamond fluorescence. The samples were glued onto a translation stage and the fluorescence from the NV centers were collected by either a spectrometer for time-averaged spectroscopy or a Single Photon Counting

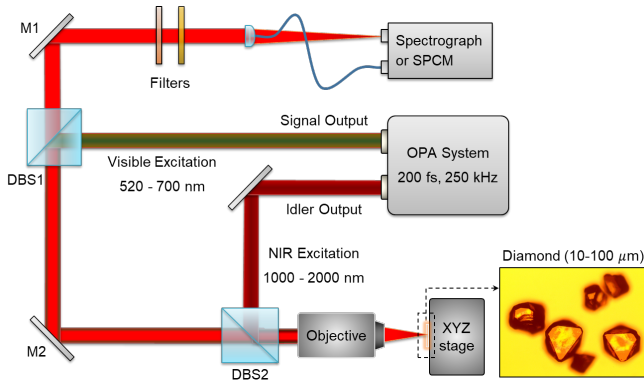


Figure 1. An OPA system served as a tuneable light source, providing 200 ps excitation pulses at 250 kHz repetition rate. The “signal” and “idler” outputs of the OPA were directed onto the sample optical path using dichroic beam splitters (DBS1 and DBS2). Additional bandpass filters and longpass filters were placed along the “signal” and “idler” paths respectively to get rid of any light leaking from the OPA’s own pump source (800 nm). Laser paths for the different wavelength regions were blocked or opened as needed in the experiments. The photoluminescence can be directed into a spectrometer or a Single Photon Counting Module (SPCM) for lifetime measurements.

Module (SPCM) for time-correlated measurements. The trigger of the single photon counter was sourced from the 250 kHz repetition rate of the OPA pump and counts were recorded by a (PicoHarp 300) dual-channel counter. A bandpass filter centered at 582 nm wavelength with a 75 nm bandwidth and a 650 nm longpass filter were placed along the collection path when distinguishing between the NV^0 and NV^- photoluminescence respectively.

RESULTS

Power Dependence

To identify multi-photon excitation generated PL from NV centers, we compared the power dependence of collected PL with pulsed excitation centered at 535 nm with excitation centered at 1276 nm, half the NV^- ZPL energy in Figure 2(a) and (b). The integrated counts from the spectrally resolved fluorescence for NV^0 (550-620 nm) and NV^- (650-800 nm) as a function of power is fitted with a power law to the n^{th} power. The emission intensity from the 535 nm excitation as a function of pump power yields a clear linear dependence ($n=1.01\pm0.05$ for NV^- and $n=1.13\pm0.07$ for NV^0) as shown in Figure 2(a). The NV^- fluorescence follows mainly a quadratic dependence $n=2.10\pm0.18$ while the NV^0 fits a cubic power law $n=3.00\pm0.34$ for 1276 nm excitation. The uncertainty δn of the n^{th} power is the standard deviation of several trials for the corresponding excitation wavelength.

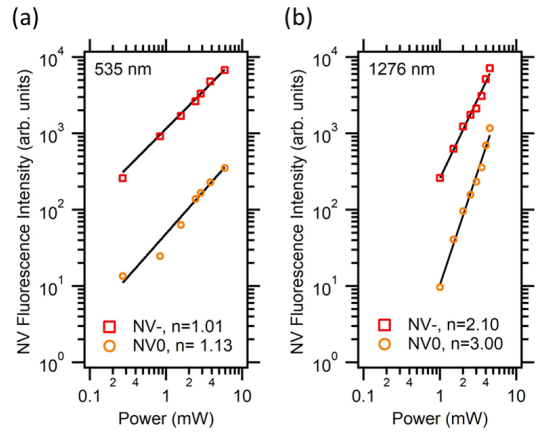


Figure 2. Power dependence of NV^0 and NV^- fluorescence intensities at (a) 535nm and (b) 1276nm excitation wavelengths. The solid lines are power law fits with n as the power parameter.

Figure 3 looks at how the near-infrared excitation affects the spectral profile of the NV system. NV fluorescence spectrum and corresponding NV^- to NV^0 ratio under 1060 nm or 1210 nm excitation have been displayed in a series of excitation powers. At 1060 nm excitation, two photons have enough energy to excite both the NV^- and NV^0 charge states, while past 1150 nm, e.g. 1210 nm, an additional photon is needed to reach the excited state of NV^0 . Figure 3(a),(b) shows an increase in NV^0 component, or equivalently a decrease in NV^- to NV^0 ratio, with increasing excitation power. Longer excitation wavelengths past 1210 nm show more NV^- than NV^0 . It is clear that irrespective of excitation wavelength, the NV^0 component increases with pump power, e.g. Figure 3(c), albeit at lesser rates for longer wavelengths. Our multi-photon data indicates an increased ionization of NV^- due to a higher illumination power, which pushes the dynamic balance between two NV charge state populations towards NV^0 . The result is in agreement with the previous reports for single photon excitation [10].

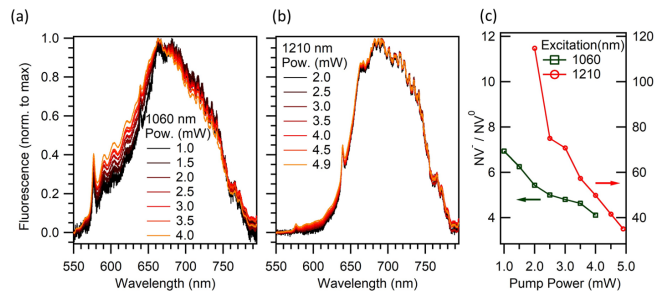


Figure 3. Fluorescence of NV diamond at various pump powers for (a) 1060 nm excitation, (b) 1210 nm excitation and their corresponding NV^- to NV^0 ratio (c).

Spectrum and Lifetime

Following the same diamond centers, we looked at the wavelength dependence of the spectral profile. Figure 4(a) shows representative room temperature fluorescence spectra of the NV centers at various excitation wavelengths. Our results indicate that NV centers can be excited continuously from 1050 nm to 1300 nm with varying efficiency for each of the different charged states. Using appropriate bandpass filters, we collect the integrated fluorescence intensity of the NV^- charge state (750-800 nm) and the NV^0 charge state (550-620 nm) separately as a function of pulsed excitation wavelength. The integrated intensity for each charge state and the ratio between them is shown in Figure 4(b). If an energy equivalent of two excitation photons is assumed, the emission intensity at these excitation wavelengths is consistent with the characteristic absorption cross-sections or photoluminescence (PLE) spectra of NV^- with conventional single-photon excitation [11]. For example, in our data the intensity in fluorescence emission peaks at around 1070 nm corresponding to twice the wavelength where single photon absorption peaks (535 nm) in diamond NV [12]. The inefficient pumping of the NV^0 charge state with wavelengths longer than the ZPL of the NV^0 (575 nm), is reflected in the decrease in fluorescence intensity as function of pump wavelength across 1150 nm towards longer wavelengths shown in Figure 4(b). The fluorescence intensity of the NV^0 charge state ensemble goes down as well but, nonetheless, remains non-zero. A notable feature is the increase in intensity ratio (NV^-/NV^0) of the charged states toward longer wavelengths. Within the excitation wavelength range in our experiments, the relative NV^- emission and excitation is much more efficient at wavelengths beyond 1150 nm.

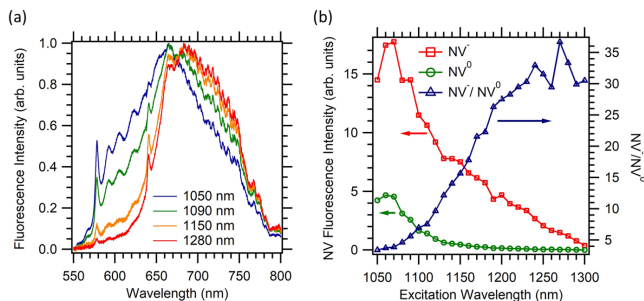


Figure 4. (a) Representative PLE spectra of NV centers at 1050 nm, 1090 nm, 1150, and 1280 nm. The fluorescence spectra are normalized to maximum intensity. (b) Integrated intensity of NV^0 (550-620 nm) and NV^- (650-800 nm) from spectra, e.g. Figure 4(a), versus excitation wavelength. The ratio between NV^- and NV^0 intensities is also shown in the graph.

We also compared the NV ratio between single photon (510 nm, 550 nm) and two-photon excitation (1060 nm)

as shown in Figure 5(a). Due to the laser light's proximity to the fluorescence region, a long pass filter with cut-off at 600 nm is placed in the collection path to filter out the laser reflections from the sample when exciting at 550 nm. The effect of the long pass filter is manifested in the loss of fluorescence information below 600 nm for the 550 nm excitation. Nonetheless, the reduction of NV^0 with respect to NV^- is qualitatively apparent compared to 510 nm or 1060 nm excitation. Within the single photon excitation range, longer wavelength yields increasing NV^- intensity with respect to NV^0 as seen when comparing 510 nm excitation with a 550 nm excitation which is consistent with the absorption spectra of the charged states [12]. Also, one can clearly see from Figure 5(a) that near-IR excitation contains relatively more NV^0 component than NV^- .

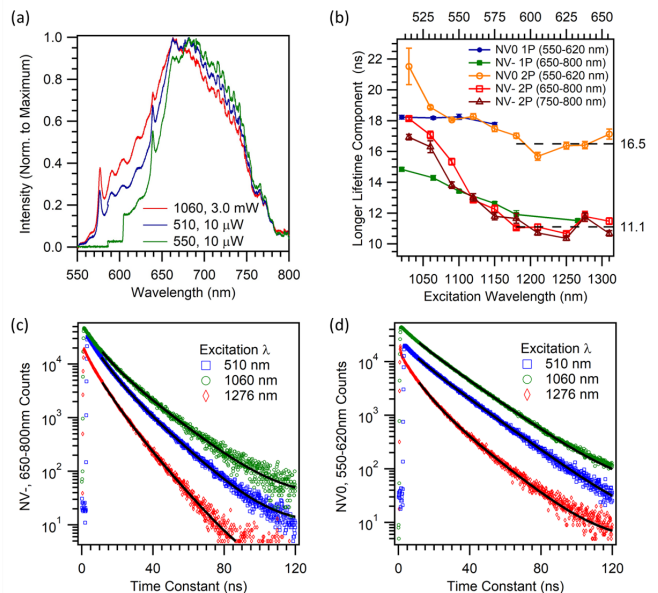


Figure 5. (a) Fluorescence comparison of single photon excitation (510 nm and 550 nm) with multi-photon excitation (1060 nm). Graph (b) compares the lifetime when exciting with single photons and multiple photons. The top axis corresponds to one-photon (1P) excitation wavelength while the bottom axis corresponds to the two-photon (2P) excitation wavelength. For the multiple-photon excitation, the NV^- fluorescence is taken at two wavelength windows for comparison. The fluorescence decay is fitted with a bi-exponential function. The longer lifetime or slower decay component is plotted for various excitation wavelength. Not included in the figure is the shorter lifetime or faster decay component, also observed, in single photon excitation which is simply consistent at around 7 ns. Representative decay plots and bi-exponential fits for (c) NV^- and (d) NV^0 fluorescence comparing 510 nm, 1060 nm, and 1276 nm excitation wavelengths are also shown above.

The decay of the fluorescence is also recorded at various wavelengths. A bi-exponential function provides a better fit to our data than a single exponential and takes into

account the presence of any extraneous, short-lived luminescent defects. The lifetime of the long-lived component is plotted in Figure 5(b) showing both the NV charged state lifetime at various frequencies of multi-photon (MP) excitation in as well as a control measurement using one-photon (1P) excitation. Note that there is a noticeable change in the lifetime from shorter to longer excitation wavelength which eventually flattens beyond 1150 nm excitation or its single-photon equivalent. Although the downward trend is not universally reported by other groups so far, our findings are not unique. Reference [13] reported a similar downward trend in 30% of their investigated nanodiamonds using conventional single-photon excitation. To rule out the possibility of leakage from strong NV⁰ emissions at shorter wavelength excitation, the multi-photon excitation NV⁻ fluorescence is taken at two wavelength windows for comparison, one in the 650-800 nm interval and the other at 750-800 nm interval. The consistently higher time constant of the 650-800 nm fluorescence window of the NV⁻ at excitations shorter than 1150 nm is indicative of some NV⁰ fluorescence leaking into the NV⁻ collection window. Beyond 1150 nm, the NV⁰ emission is less intense minimizing possible leakage effects. We then can take the time constant beyond this excitation wavelength to be the NV⁰ lifetime 16.5 ± 0.6 ns and NV⁻ lifetime 11.1 ± 0.4 ns, which are within the range reported by other groups. Compared to the measurements from 1P experiments, the 1P lifetime tends to agree with 2P result at long excitation wavelength. In addition, an interesting observation is the slow downward trend of lifetime as a function of excitation wavelengths for 1P case compared to 2P case. This is possibly why the observation of the downward trend was not universally reported before. Our result strongly suggests other mechanisms are involved in multiple-photon excitation that leads to a dependence of lifetime in excitation wavelength.

The faster decay component has a lifetime around ~ 7 ns for both 2P and 1P excitations. The fast decay does not vary much with excitation wavelength. One explanation for the fast decay can be another luminescent defect as mentioned before. Another explanation can be the quenching effect of NV PL due to nearby neutral substitutional nitrogen defects N_s⁰ [14, 15]. The N_s⁰ can be located at a range of distances around NV centers. If one thinks of the NV center and N_s⁰ as a donor-acceptor pair, the energy transfer rate between the pair will depend on the distance between them [16]. Such phenomena leads to non-single exponential decay. These non-single exponential decays are also observed in nanodiamonds, e.g.[17].

DISCUSSION

Experimentally, the two-photon absorption (2PA) cross-section is related to the detected PL counts [18]

$$\sigma_2 \approx \frac{Ff\tau}{1.28\phi C\eta n\lambda P^2} \quad (1)$$

where F is in units of photon/s; ϕ is the PL collection efficiency of the experimental system; η is the quantum yield of the defect; C is the density of the defects, λ is the excitation wavelength in vacuum; n is the refractive index of the media; P is the average laser power; τ is the pulse duration; f is the repetition rate; and σ_2 is the 2PA cross-section in units of GM , where $1 GM = 10^{-50} \text{ cm}^4 \cdot \text{s}/\text{photon}$.

The NV⁻ 2PA cross-section $\sigma_2(\lambda)$ from 1050nm to 1280nm excitation can be estimated from our PLE data. Considering our laser linewidth is ~ 30 nm, we use the measured 2PA cross-section at 1064nm from reference [6] as our calibration for the 1060nm excitation such that $\sigma_2(1060) \approx 0.45 \pm 0.23GM$. Assuming the experimental conditions remained fixed during the PLE measurement as the excitation wavelength is changed, then the 2PA cross-section $\sigma_2(\lambda)$ can be simplified to

$$\sigma_2(\lambda) = \frac{1060}{\lambda} \frac{F(\lambda)}{F(1060)} \sigma_2(1060). \quad (2)$$

Figure 6 shows our estimate of the 2PA cross-section for NV⁻ center at different excitation wavelength based on our PLE measurements. The 2PA cross-section agrees with the reported one-photon absorption(1PA) by reference [12] at room temperature. The missing resonance at 1150nm is possibly due to the our broad laser linewidth. Low temperature experiment and narrower laser linewidth will help to explore the resonance in the future.

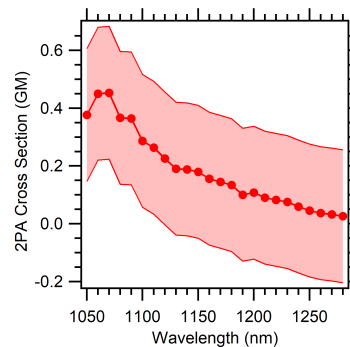


Figure 6. NV⁻ 2PA absorption cross-section calculated from our PLE data based on the measured 2PA cross-section and error at 1064nm excitation from reference [6].

The schematic of the negative and neutral state shown in Figure 7 maps our understanding of the behavior of the system. The energy level of the states and band

offsets follows reference [12] which is the most consistent with our results. From the schematic, we can see that an excited negatively charged state NV^{-*} could absorb another photon, 0.65 eV or higher, to raise the electron out to the conduction band. Hence, if an NV^{-} state absorbs three photons, each photon at half the energy of the NV^{-} ZPL, it can be converted into the excited state of NV^0 . If the total transition energy is attained, a direct three-photon absorption of an NV^0 electron from the ground state will also get the system to its excited state (NV^{0*}).

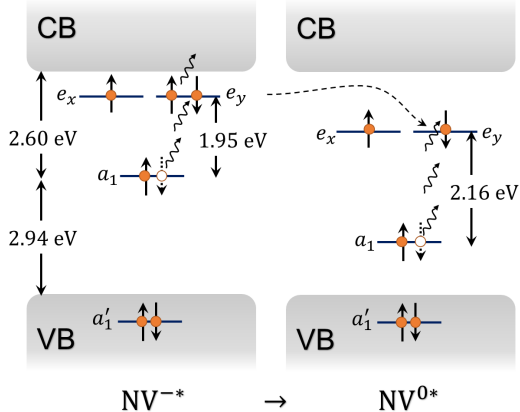


Figure 7. A two-photon, three-photon excitation of NV^{-} and NV^0 respectively leaving them in their excited states (*). An excited negatively charged state NV^{-*} could absorb another photon to raise the electron out to the conduction band. If an NV^{-} state absorbs three photons with a total energy of 2.60 eV, it is converted into the excited state of NV^0 . A direct three-photon absorption of an NV^0 electron from the ground state will leave it in its excited state (NV^{0*}) if the total photon energy is greater than or equal to 2.16 eV.

The power dependence of the NV^{-} and NV^0 charged states with 1276 nm excitation provides evidence for a multi-photon procedure or a series of pathways for the NV electronic transitions. For the negatively charged state, a two-photon excitation or absorption is the most straightforward interpretation based on its quadratic power dependence. The cubic dependence of the NV^0 PL intensity on the other hand may have two possibilities. The mechanism for these is illustrated in Figure 7. The first is a direct absorption of three photons 1276 nm photons to reach the excited state. Note that three times the energy of a 1276 nm photon, for a total of 2.92 eV, is more than enough to reach the 2.16 eV needed to excite the NV^0 . The second possible explanation is an NV^{-} to NV^0 conversion. One such conversion mechanism was proposed by Beha et al.[12] and Shiyushev et al.[5] whereby an excited NV^{-} state absorbs another photon into the conduction band followed by an Auger process that releases enough energy to remove the defect charge. Later work, e.g. [12], on photo-induced ionization dynamics did not invoke the Auger process. The

NV^{-} ionization energy was concluded, per Ref.[12], to be only 2.6 eV. We point out that the three 1276 nm photons have more than enough energy required for an NV^{-} electron to reach the conduction band from the NV^{-} ground state.

We also point out that the two-photon process is more efficient for exciting the NV^0 state than the NV^{-} compared to excitation at the single photon equivalent energy (Figure 5(a)). This is likely due to excitation pulses which have higher peak power inducing faster charge state conversion from NV^{-} to NV^0 compared with continuous-wave (CW) pumping.

CW, green laser in tandem with a 650nm long pass filter is often used for NV^{-} , single-photon related experiments. However, this strategy is not effective in filtering out the NV^0 emission as demonstrated in Figure 5(b). A longpass filter with a much longer wavelength cutoff is needed to significantly reduce the fluorescence overlap between the two charge states. Alternatively, our multi-photon experiment showed that the NV^{-} charge state can also be prepared with higher fidelity using excitation wavelength >1150 nm compared to shorter, near-infrared wavelengths at the same illumination power.

The NV^{-} 's slower or longer decay component, Figure 5(b), shows a decreased lifetime when excited at wavelengths greater than 1150 nm compared to when excited at wavelengths shorter than 1150 nm. In part, this can be attributed to some NV^0 fluorescence leaking into the NV^{-} collection window. The leakage effect is supported by a consistently longer time constant for NV^{-} fluorescence collected at 650-800 nm as compared to a 750-800 nm collection window. The effect can partially explain the leveling of the time constant at >1150 nm pumping due to an inefficient two-photon excitation of NV^0 at these wavelengths. Less NV^0 leaks into the NV^{-} collection window, unless the pump power is increased whereby 3-photon processes starts to dominate and NV^0 population recovers.

The longer lifetime component for NV^0 decay for excitation wavelengths shorter than 1150 nm is indicative of multiple processes feeding into NV^0 population. Diamond fluorescence in a series of excitation powers and wavelengths and their corresponding NV^{-} to NV^0 ratio also show that there is a significant number of carriers feeding into the NV^0 states at higher powers and for wavelengths shorter than 1150nm (half the energy of NV^0 ZPL). It is possible that this may be due to conversions from NV^{-} to NV^0 , excitation of defects and quenching of PL due to other defects in the vicinity. The dependence of the lifetime with wavelength would be better understood using a streak camera which is within purview of future work.

CONCLUSION

We have shown that near-IR excitation of NV centers, resonant at half the energies of the NV states and wavelengths within the vicinity (1050 to 1300 nm) is allowed through a multi-photon process. Preferential population of NV^- or NV^0 is achieved by tuning to an appropriate wavelength or excitation power. In general, longer wavelength and lower power is required to have more NV^- population and vice versa for populating NV^0 . We note that excitation at low energy is extremely useful for biomedical imaging applications since infrared light can penetrate deep into biological tissues with little scattering or damage [19]. Another important application is in spin-photon entanglement experiments. NV centers can be prepared in an entangled state between a single photon and the $m_s = \pm 1$ electronic spin of an NV center [20]. Following selective resonant excitation to the A_2 state, the system decays into one of the spin states, simultaneously emitting a circularized polarized photon which is orthogonal to the photon emitted when an electron decays to an opposite spin state. Isolating this photon emission is significantly challenging due to the difficulty in extinguishing the resonant excitation pulse back into the detector. A near-IR excitation would widely separate the excitation and emission wavelength, thereby increasing signal contrast for the entangled photon emission.

ACKNOWLEDGMENTS

R. Balili wants to thank the Michigan Space Grant Consortium (MSGC) seed grant and the Calvin Alumni Association (CAA) for the equipment funding and travel grants that made this collaboration possible. P. Ji was supported by the Charles E. Kaufman New Initiative grant and NSF grant PHY-1540879. G. Dutt acknowledges DOE grant no.DE-8C-0006638 for materials, equipment, and financial support. We also acknowledge Dr. Arfaan Rampersaud for the helpful discussions and Columbus Nanoworks Inc. for the diamond samples.

* Corresponding author email address: pej13@pitt.edu

† Corresponding author email address: rbb5@calvin.edu

‡ Corresponding author email address: gdutt@pitt.edu

- [1] A. Gruber, A. Dräbenstedt, C. Tietz, L. Fleury, J. Wrachtrup, and C. v. Borczyskowski, *Science* **276**, 2012 (1997).
- [2] F. Jelezko, T. Gaebel, I. Popa, M. Domhan, A. Gruber, and J. Wrachtrup, *Phys. Rev. Lett.* **93**, 130501 (2004).
- [3] M. W. Doherty, N. B. Manson, P. Delaney, F. Jelezko, J. Wrachtrup, and L. C. Hollenberg, *Physics Reports* **528**, 1 (2013).
- [4] R. Schirhagl, K. Chang, M. Loretz, and C. L. Degen, *Annual Review of Physical Chemistry* **65**, 83 (2014), pMID: 24274702.
- [5] P. Siyushev, H. Pinto, M. Vörös, A. Gali, F. Jelezko, and J. Wrachtrup, *Phys. Rev. Lett.* **110**, 167402 (2013).
- [6] T.-L. Wee, Y.-K. Tzeng, C.-C. Han, H.-C. Chang, W. Fann, J.-H. Hsu, K.-M. Chen, and Y.-C. Yu, *The Journal of Physical Chemistry A* **111**, 9379 (2007).
- [7] P. Ji and M. V. G. Dutt, *Phys. Rev. B* **94**, 024101 (2016).
- [8] D. A. Hopper, R. R. Grote, A. L. Exarhos, and L. C. Bassett, *Phys. Rev. B* **94**, 241201 (2016).
- [9] I. P. Ivanov, X. Li, P. R. Dolan, and M. Gu, *Opt. Lett.* **38**, 1358 (2013).
- [10] N. Manson and J. Harrison, *Diamond and Related Materials* **14**, 1705 (2005).
- [11] G. Davies and M. F. Hamer, *Proceedings of the Royal Society of London A: Mathematical, Physical and Engineering Sciences* **348**, 285 (1976).
- [12] K. Beha, A. Batalov, N. B. Manson, R. Bratschitsch, and A. Leitenstorfer, *Phys. Rev. Lett.* **109**, 097404 (2012).
- [13] J. Storteboom, P. Dolan, S. Castelletto, X. Li, and M. Gu, *Opt. Express* **23**, 11327 (2015).
- [14] G. Liaugaudas, A. T. Collins, K. Suhling, G. Davies, and R. Heintzmann, *Journal of Physics: Condensed Matter* **21**, 364210 (2009).
- [15] G. Liaugaudas, G. Davies, K. Suhling, R. U. A. Khan, and D. J. F. Evans, *Journal of Physics: Condensed Matter* **24**, 435503 (2012).
- [16] J. R. Lakowicz, *Principles of Fluorescence Spectroscopy*, 3rd ed. (Springer, 2006).
- [17] J. Tisler, G. Balasubramanian, B. Naydenov, R. Kolesov, B. Grotz, R. Reuter, J.-P. Boudou, P. A. Curmi, M. Sennour, A. Thorel, M. Borsch, K. Aulenbacher, R. Erdmann, P. R. Hemmer, F. Jelezko, and J. Wrachtrup, *ACS Nano* **3**, 1959 (2009), pMID: 21452865, <https://doi.org/10.1021/nn9003617>.
- [18] C. Xu and W. R. Zipfel, *Cold Spring Harbor protocols* **2015** **3**, 250 (2015).
- [19] S. L. Jacques, *Physics in Medicine and Biology* **58**, R37 (2013).
- [20] E. Togan, Y. Chu, A. S. Trifonov, L. Jiang, J. Maze, L. Childress, M. V. G. Dutt, A. S. Sorensen, P. R. Hemmer, A. S. Zibrov, and M. D. Lukin, *Nature* **466**, 730 (2010).